HEFAT2010
7th International Conference on Heat Transfer, Fluid Mechanics and Thermodynamics
19-21 July 2010
Antalya, Turkey

TWO-CYLINDER WAKE WITH AND WITHOUT TRIPWIRES

Md. Mahbub Alam and J.P. Meyer
Department of Mechanical and Aeronautical Engineering
University of Pretoria, Pretoria 002, South Africa

ABSTRACT

This works aims to investigate interference between two tripped cylinders of identical diameter D (= 49 mm), based on measured time-mean drag (C_D) and fluctuating drag (C_{Df}) and lift (C_{Lf}) at stagger angle $\alpha = 0^\circ \sim 180^\circ$ and gap spacing ratio $T/D = 0.1 \sim 5$, where T is the gap width between the cylinders. Two tripwires, each of 5 mm, were attached on each cylinder at azimuthal angle $\beta = \pm 30^\circ$. Forces on two plain cylinders are also measured and compared with those on tripped cylinders. Flow visualization test was conducted to observe flow structures around the cylinders. C_D, C_{Df} and C_{Lf} all for the plain cylinders are strong function of α and T/D due to strong mutual interference between the cylinders, connected to nineteen distinct flow categories including three kinds of tristable flow and five kinds of bistable flow. On the other hand, the tripped cylinders interfere weakly one another, resulting in insignificant variation in forces with α and T/D. Tripwires suppress forces on the cylinders remarkably.

INTRODUCTION

In a real life architectural environment, most buildings and structures are in close proximity of each other, such as chimney stacks, tube bundles in heat exchangers, overhead power-line bundles, bridge piers, stays, masts, chemical-reaction towers, offshore platforms and adjacent skyscrapers. The alternate shedding of vortices in the near wake leads to fluctuating forces on the structures and may cause structural vibrations, acoustic noise, or resonance, which in some cases can trigger failure. Aerodynamics of two closely separated structures is of both fundamental and practical significance. Two cylinders are considered as the basic model to understand the physics of flow around multiple structures. Fluid forces, Strouhal numbers (St) and flow structures are the major factors considered in the design of multiple slender structures subjected to cross flow. The flow around two cylinders is apparently more complicated than that around a single one.

Based on the interference effect between two cylinders, Zdravkovich [1] divided the whole region of possible arrangements of two cylinders into four; (i) the proximity interference region, where the flow around one cylinder affects the other; (ii) wake interference region, the near-wake flow of the upstream cylinder is unaffected by the downstream one; however, the downstream one is significantly affected by the upstream cylinder; (iii) the proximity and wake interference region includes the combination of the proximity and wake interferences; (iv) the no interference region, where the wake of one cylinder does not affect the other. This classification is useful from the engineering design point of view, though providing little information on the flow structure around the cylinders.

Time-averaged drag and lift forces acting on two staggered cylinders have been examined in literatures (e.g., [2, 3]). However, data in the literatures are mostly concerned

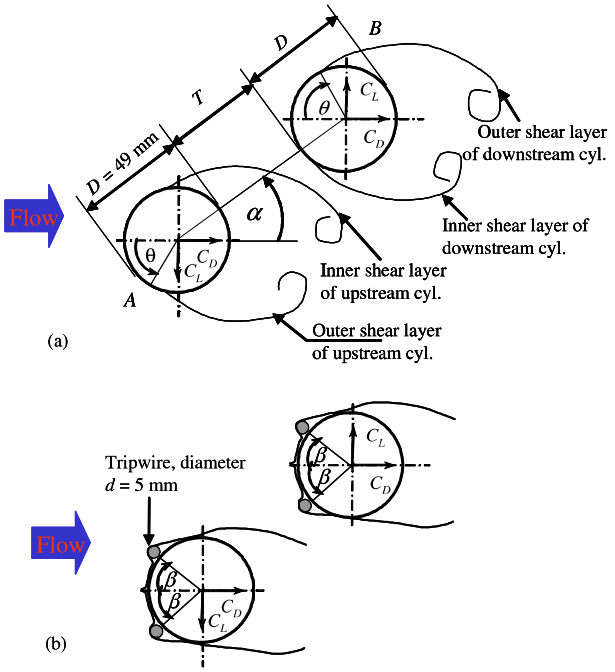

Figure 1 Definitions of symbols and arrangement of cylinder (a) without tripwires, (b) with tripwires.

with the downstream cylinder. Though the fluctuating lift and drag forces acting on structures are a major cause of the fatigue failure of the structures and are used for predicting flow-induced responses, a review of literatures indicated that the information on fluctuating lift and drag forces on either cylinder is very limited, and many aspects of the flow structure around two staggered cylinders have yet to be explored. Furthermore, no methods have been developed to reduce forces on and interference between two cylinders in staggered configurations. Use of tripwires to control boundary layer on a cylinder is interesting and effective [4]. Alam et al. [5] used tripwires as control objects to suppress forces on two cylinders in tandem and side-by-side configurations.

The objectives of this study were to (i) measure interference-induced time-averaged drag coefficient (C_D), fluctuating drag coefficient (C_{Df}) and fluctuating lift coefficient (C_{Lf}) and St, for two plain cylinders, (ii) elucidate the flow structure around and behind the cylinders, (iii) classify force region on T/D-α plane, and (iv) reduce forces on and inference between the cylinders using tripwires, where T is the gap width between the cylinders, D is the diameter of a cylinder and α is the stagger angle. Measurements were conducted at $\alpha = 0^\circ$ ~ 180°, T/D = 0.1 ~ 5.0. The linkage between force and flow structure and the interactions between the cylinders are discussed in details.

EXPERIMENTAL DETAILS

Measurements were done in a closed-circuit wind tunnel with a test section of 1.20×0.30m at the fluid mechanics laboratory of Kitami Institute of Technology, Japan. The Reynolds number (Re) based on the diameter of a single cylinder was 5.52×10^4 and the turbulent intensity was 0.5%. C_D, C_{Df} and C_{Lf} were measured using two load cells installed inside a circular cylinder of diameter D =49 mm (see Alam et al. [6] for details of the load cell). St was estimated from spectral analysis of fluctuating pressure measured on side surfaces of the cylinders. Two tripwires, each of 5 mm were placed at azimuthal angle $\beta = \pm30^\circ$ measured from front stagnation point. Experiments were performed at $\alpha = 0^\circ$, 10°, 25°, 45°, 60°, 75°, 90°, 105°, 120°, 135°, 155°, 170°, and 180°, for T/D =0.1 ~ 5. Flow visualization was carried out at Re = 350 in a water channel with a 250 mm × 350 mm working section and 1.5 m long. In the flow visualization test, two circular cylinders with identical diameter of 20 mm were used.

RESULTS AND DISCUSSION

Force on the cylinders

Contours of C_D, C_{Df} and C_{Lf} on a T/D-α plane are shown in Fig. 2-4 for the cases of the plain and tripped cylinders. Here tripped cylinders mean cylinders with tripwires. In the scale bars, the color or the range marked by '*' and '♠' indicates the value of a single isolated plain and tripped cylinders, respectively. For the purpose of simplicity, the result can be described with reference to Fig. 1, in which the cylinder A is tentatively assumed to be fixed, and thus the two parameters T/D and α suffice to determine the arrangement of the two cylinders. It may be noted that the cylinder B is the downstream cylinder for $-90^\circ<\alpha<90^\circ$ and it becomes the upstream cylinder for $90<\alpha<-90^\circ$, i.e., the left and right sides of a contour map show the values of coefficient of the upstream and downstream cylinders, respectively. At the peripheries of the inner and outer circles, the values of T/D are 0 and T/D=5.0, respectively. Note that the values of C_D, C_{Df}, C_{Lf} and St of a single plain cylinder are 1.12, 0.14, 0.48 and 0.186, respectively. Repulsive C_L is considered as positive (Fig. 1).

The contour maps show that C_D, C_{Df} and C_{Lf} of the plain cylinders briskly vary with change in T/D and α (Figs. 2a, 3a, 4a). However, those of the tripped cylinders vary rather mildly. The observation suggests that interference between

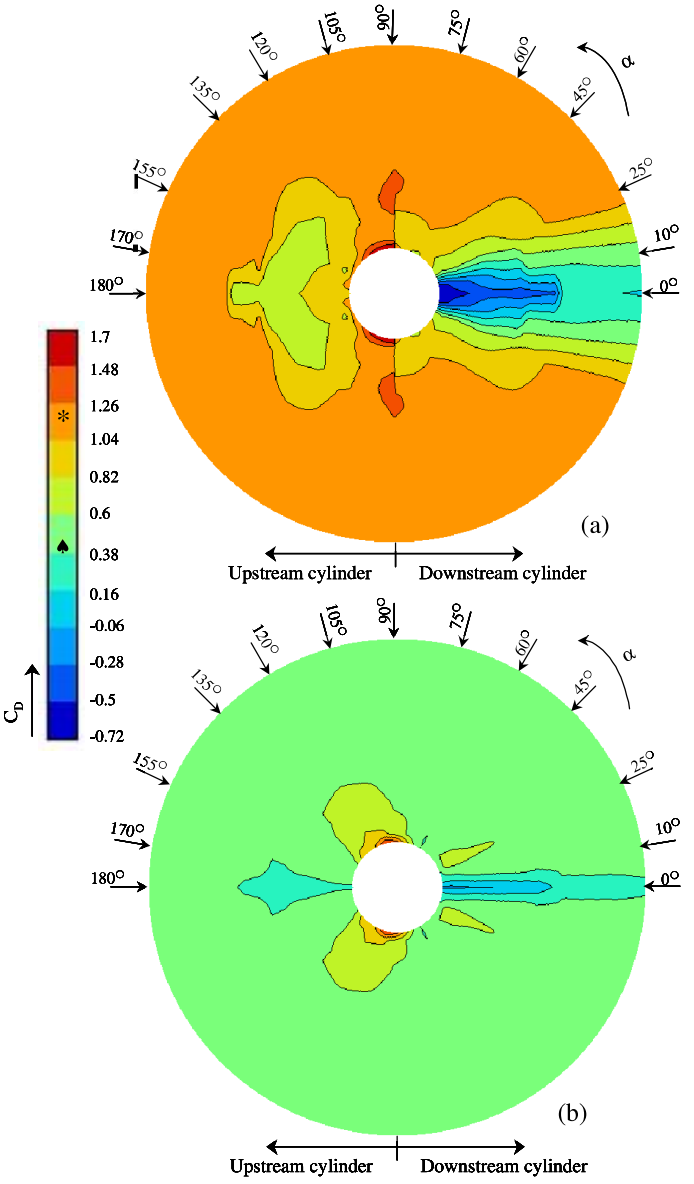

Figure 2 Contour plot of time averaged drag coefficient, C_D: (a) plain cylinders, (b) tripped cylinders. '*' and '♠' denotes C_D values of a single cylinder plain and tripped, respectively.

the plain cylinders is much strong but that between the tripped cylinders is weak. For the case of plain cylinders, it is seen that the upstream cylinder experiences somewhat lower C_D at α = -120°~120°, T/D<3.0 than a single isolated cylinder (Fig. 2a). The downstream cylinder experiences highly negative C_D at α = -10°~10°, T/D<3.0, with a maximum negative value of -0.72 when it is in contact with the upstream cylinder at α=0°. Maximum C_D acts on the two cylinders when they are arranged in side-by-side with

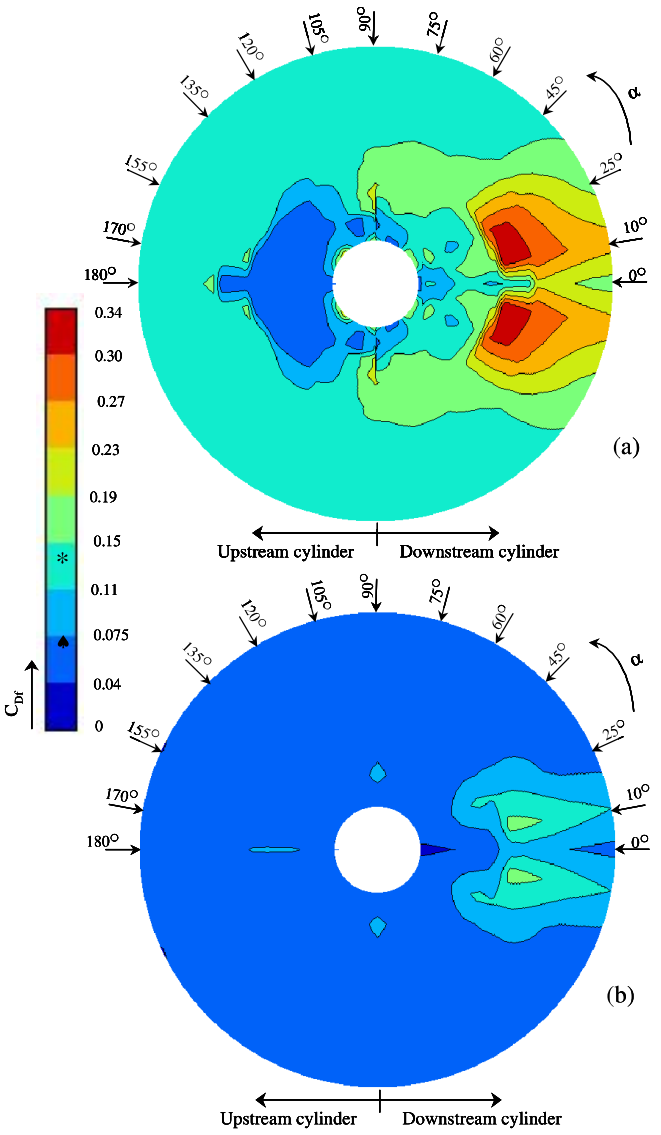

Figure 3 Contour plot of fluctuating drag coefficient, C_{Df}: (a) plain cylinders, (b) tripped cylinders. '*' and '♠' denotes C_{Df} values of a single cylinder plain and tripped, respectively.

T/D=1.2~2.0 in which an enhanced antiphase vortex shedding occurs from the cylinders. A significantly higher C_D acts on the upstream cylinder at ±90°<α<±120°, T/D<0.2. For the case of tripped cylinders, a significant reduction in C_D is observed over the whole region except the region bounded by T/D<0.2, α=90°~105° where color is still red. In this region, however, C_D can be reduced by changing the positions of the outer tripping wires toward the forward. Value of C_D on the most of the region is 1.04~1.26 (Fig. 2a) which have been suppressed to 0.38~0.6 by using tripping wires (Fig. 2b). On average, the suppression in C_D is about 58%. Figure 2(b) indicates that mutual interference between the cylinders is greatly weakened when tripping wires are used on the cylinders, which was an objective of this study.

For the case of plain cylinders, significantly higher magnitudes of C_{Lf} and C_{Df} act on the downstream cylinder at α = -35°~35°, T/D>2.5 (Figs. 3a, 4a). C_{Lf} and C_{Df} on the upstream cylinder become extremely small for α = -120°~120°, T/D<3.0 and on both cylinders in the vicinity of side-by-side arrangement at small T/D. In the first region, they become very small because formation of fully developed Karman vortex behind the upstream cylinder is retarded by the presence of the downstream cylinder [6]. In the second region, the gap flow between the cylinders acts as a base bleed, propelling the rolling positions of the outer shear layers downstream, causing small C_{Lf} and C_{Df}.

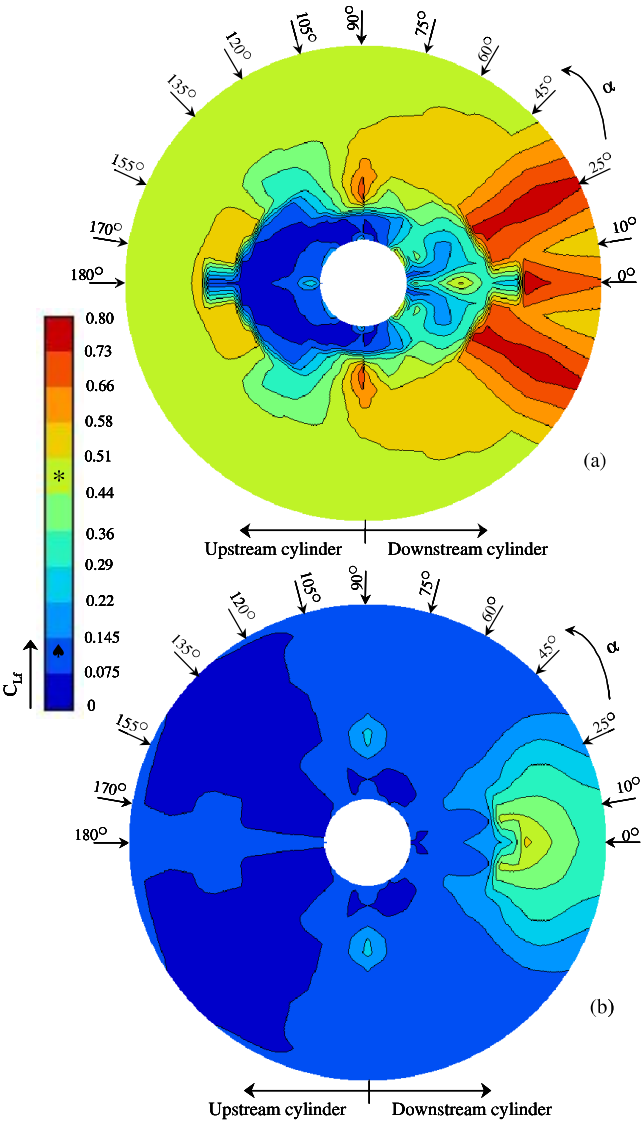

Figure 4 Contour plot of fluctuating lift coefficient, C_{Lf}: (a) plain cylinders, (b) tripped cylinders. '*' and '♠' denotes C_{Lf} values of a single cylinder plain and tripped, respectively.

C_{Df} of the tripped cylinders is suppressed to very small value for the whole region, compared that of the plain cylinders. The value of C_{Df} in the region α=10°~25°, T/D=2.5~3.5 is maximum 0.30~0.34 for the plain cylinders and reduces to 0.15~0.19 when tripping wires are used. Here also mutual interference effect between the tripped cylinders is very small. A dramatic decrease in C_{Lf} is self-evident for tripped cylinders compared to plain cylinders (Fig. 4b). C_{Lf} in the red region (maximum values of C_{Lf}) of the plain cylinders has been reduced to significantly small value by the tripping wires on the cylinders. Thus use of tripping wires on two cylinders is an effective means for suppressing interference between and forces acting on two cylinders in any arrangements.

Classification of force region and flow structures

In the previous section, variation in C_D, C_{Df} and C_{Lf} with change in T/D and α has been observed brisk for the plain cylinders. On the other hand, the variation is very mild for the tripped cylinders. This implies that the wake structure as well as flow around the cylinders is strong function of T/D and α for the former case and very weakly dependent on T/D and α for the later case. Thus it would be interesting to classify the force/flow regimes for the plain cylinders first.

On the basis of magnitude and trend of C_D, mean lift C_L (not shown), C_{Df}, C_{Lf}, and St (not shown), and of characteristics of flow patterns, the entire region can be divided into nineteen small regions as illustrated in Fig. 5.

: No interference region. C_D, C_L, C_{Df}, C_{Lf}, and St are almost the same as those of a single isolated cylinder.

: Upstream-cylinder vortex suppressed region. Reduced C_D, zero C_L, very low C_{Df} and C_{Lf}; because the downstream cylinder impedes Karman vortex shedding from the upstream cylinder (Fig. 6a).

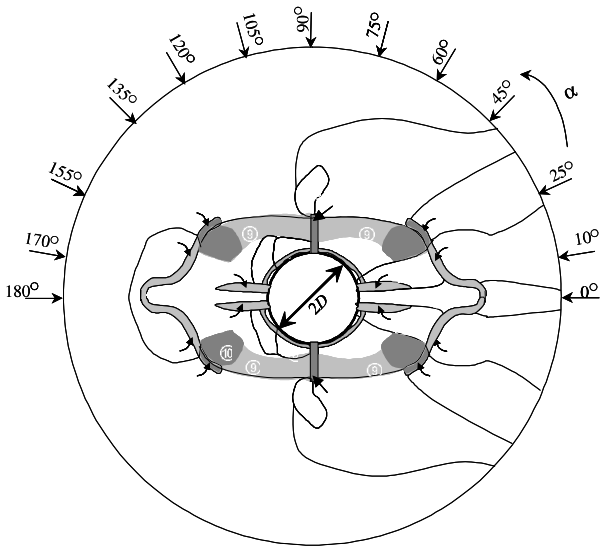

Figure 5 Sketch specifying various regions. The regions marked by shadows are multistable flow regions

: Upstream-cylinder excited flow region. Somewhat increased C_{Df} and C_{Lf}; due to appearance of fully developed and somewhat excited flow over and behind the upstream cylinder. The excitation of the flow is induced from the synchronized excited flow around the downstream cylinder (Fig. 6b).

: Highly-biased gap flow region. Attractive (negative) C_L on the upstream cylinder, low St. Highly-biased gap flow along the periphery of the upstream cylinder causes attractive C_L (Fig. 6c). The two cylinders behave like a single body causing a low St of both cylinders. This region includes a bistable flow region marked by a shadow. Intermittent formation and burst of separation bubble on the inside surface of the upstream cylinder cause such a bistable flow being responsible for a large difference in C_L on the upstream cylinder.

: Perfectly single-body region. Very high C_D, repulsive (positive) C_L and low St; the two cylinders act as a single bluff body, resulting in a high C_D and low St (Fig. 6d). Shift of stagnation point toward the gap side and a lower gradient of pressure on the inner side surface of the upstream cylinder originate the repulsive C_L. The occurrence of the lower pressure gradient is ascribed to a retardation of flow on the inner surface by the front surface of the downstream cylinder. This region also incorporates a bistable flow region marked by a shadow. A turbulent reattachment and detachment of the inner shear layer of the upstream cylinder initiates the bistable flow.

: Antiphase vortex shedding region. Very high C_D, repulsive C_L, high C_{Df} and C_{Lf}; an antiphase shedding fortifies the Karman vortices behind the two cylinders (Fig. 6e).

: Tristable flip-flopping flow region. Three modes of the flow associated with narrow wake (high St), wide wake (low St) and symmetric wake (intermediate St) are generated and switch from one to another (Fig. 6f) [7].

: Single-body-like region. Reduced C_D, C_{Df} and C_{Lf} and a single St in either wake (Fig. 6g).

: Frequency-locked bistable flow region. Reduced C_D, C_{Df} and C_{Lf} and two and one St values for the upstream and downstream cylinders, respectively. It is a bistable flow region where shedding frequency of the upstream cylinder at times locks-in to that of the downstream cylinder (Fig. 6h).

: Frequency-locked tristable flow region. Curtailed C_D, C_{Df} and C_{Lf} and two St values for the upstream and downstream cylinders. Three modes of flow with regard to vortex shedding frequencies appear intermittently. They are: (i) the flow with a high and low St for the upstream and downstream cylinders, respectively, (ii) the flow with a high St for both cylinders: lock-in of the downstream wake to the upstream one, and (iii) the flow with a low St for both cylinders: lock-in of the upstream wake to the downstream one (see [8] for details).

: Bubble-burst bistable flow region. The bistable flow results from intermittent formation and burst of a separation bubble formed on the inside surface of the downstream cylinder (Fig. 6i). The mode, in which separation bubble persists, results in a highly negative C_L on the downstream cylinder.

: Separation-bubble flow region. Highly attractive C_L, resulting from a separation bubble (Fig. 6j).

: Fully submerged flow region. Zero C_L and highly negative C_D. The downstream cylinder is fully submerged in the wake of the upstream cylinder (Fig. 6k).

: Vortex-triggered tristable flow region. The convective vortices from the upstream cylinder trigger the vortex shedding from the downstream cylinder. The modes of flow are: (i) the flow with the higher and lower *St* for the upstream and downstream cylinders, respectively, (ii) the flow with the higher *St* for both cylinders, and (iii) the flow with synchronized *St* approximately equal to that of a single cylinder. This is a transition region in which fully developed flow behind the upstream cylinder starts to be formed [8].

: Shear-layer-triggered bistable flow region. Two flow patterns appear alternately. For $\alpha=0^\circ$, i.e., in tandem arrangement, shear layers separating from the upstream cylinder reattach steadily onto the downstream cylinder or strongly roll-up behind the upstream cylinder; and for $0^\circ<\alpha<25^\circ$, only the inner shear layer of the upstream cylinder reattaches onto the front surface of the downstream cylinder or strongly rolls-up before it (Fig. 6l).

: Vortex-triggered synchronized shedding region: very high C_{Df}; in this region, the inner shear layer of the upstream cylinder rolls just before the front surface of the downstream cylinder (Fig. 6m), causing a higher fluctuation of pressure on the front surface, hence a higher C_{Df} on the downstream cylinder.

: Co-shedding flow region. Very high C_{Lf}, engendered by buffeting of upstream-cylinder vortices convective on the side-surface of the downstream cylinder (Fig. 6n) [9].

: Synchronize coupled-vortex region. Extremely high C_{Lf} and attractive C_L. The inner shear layer of the downstream cylinder sheds vortices in synchronization with the convective inner vortices from the upstream cylinder, generating a coupled vortex, resulting in a higher fluctuating pressure on the inner side surface of the downstream cylinder, hence the cylinder experiences a higher C_{Lf} (Fig. 6o).

: Small interference region: somewhat high C_{Df} and C_{Lf}; the downstream cylinder is outside the wake of the upstream cylinder, hence interference effect is trivial (Fig. 6p).

For the case of tripped cylinders, flow around the cylinders over the entire region is almost the same except $-25^\circ<\alpha<25^\circ$. The bistable or tristable flow on tripped cylinders is suppressed or their actions are insignificant. Mutual interference effect between the cylinders is reduced significantly; as a result, C_D, C_{Df} and C_{Lf} are almost insensitive to T/D and α.

As sketched in Fig. 1(b), the flow structure on the tripped cylinders has the following features: (i) shear layer

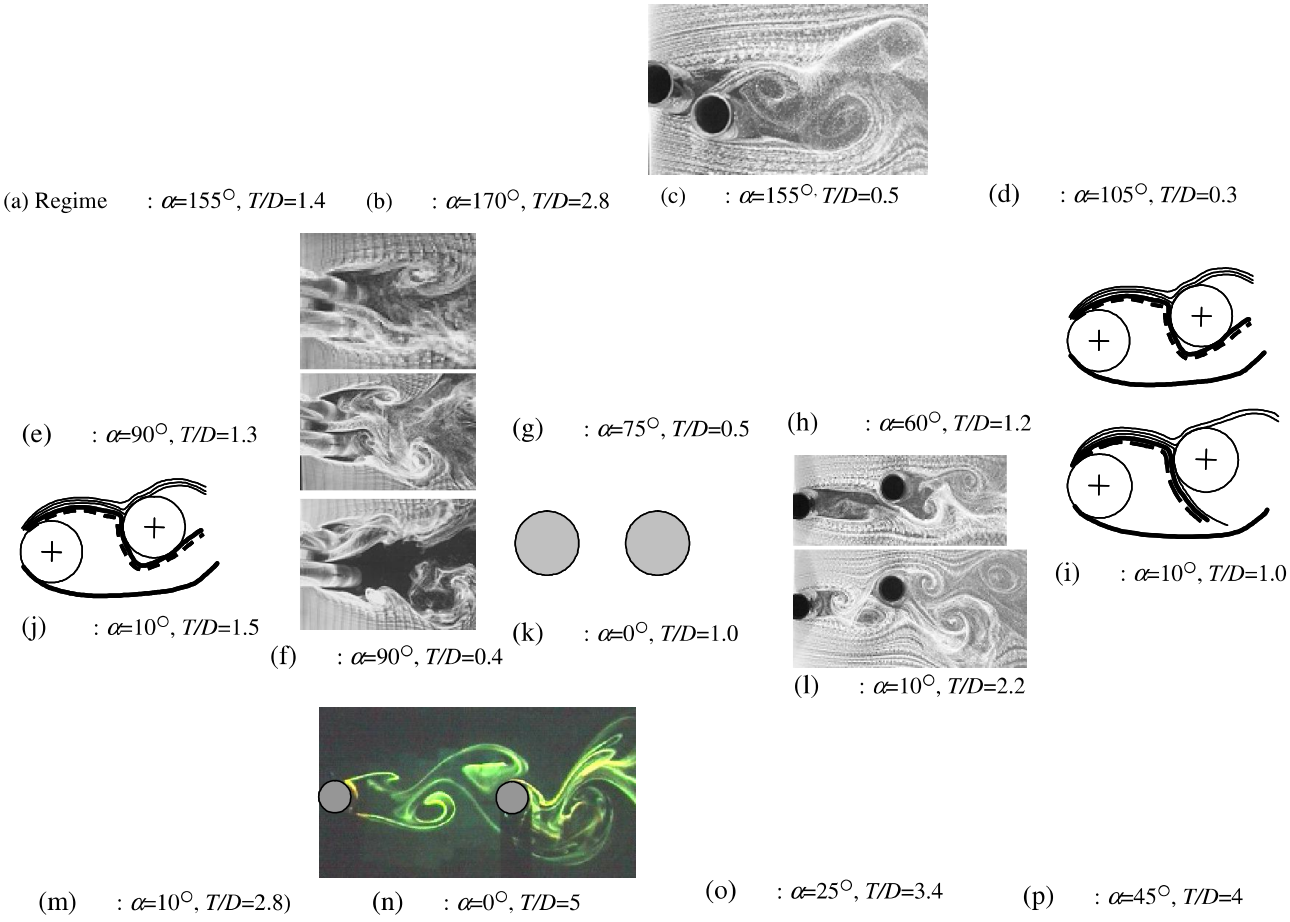

Figure 6 Representative flow structures at different regions except at , and .

separating from the tripwires reattach on the cylinder surface, (ii) the eventual separation is postponed, (iii) wake narrows, and (iv) vortex shedding is almost suppressed from the cylinders. A cylinder with the features could not interfere the other. However, for α<25°, the downstream cylinder is submerged in the wake of the upstream cylinder, hence interfered weakly.

CONCLUSIONS

The results can be summarized as follows.

(1) C_D, C_{Df} and C_{Lf} of plain cylinders are strong function of α and *T/D*, connected to nineteen distinct flow patterns, including three kinds of tristable flow and five kinds of bistable flow. The bistable or tristable flow engenders strong jumps in forces for the plain cylinders and is suppressed for the tripped cylinders or their actions are insignificant.

(2) The two plain cylinders experience maximum C_D at α = ±90°, *T/D* = 2.2 ~ 2.6 and α= ±(45°~90°), *T/D* = 1.1~1.2. Compared to plain cylinders, C_D of the tripped cylinders is suppressed by 70% in the former regime and considerably in the later regime.

(3) C_{Df}, and C_{Lf} on the downstream cylinder are extensively high in two island-like regions α = ±(10°~30°), *T/D* = 2.5~5, where the inner shear layer of the downstream cylinder sheds vortices in synchronization with the convective inner vortices from the upstream cylinder, generating a coupled vortex. Tripping wires suppress C_{Df}, and C_{Lf} by about 55% and 70%, respectively in this region.

(4) While the plain cylinders each other intervene extensively, tripped cylinders do not; hence C_D, C_{Df} and C_{Lf} are almost insensitive to *T/D* and α. Compared to the plain cylinders, the tripped cylinders experience smaller forces in the entire *T/D* and α ranges examined.

REFERENCES

[1] Zdravkovich, M.M., The effects of interference between circular cylinders in cross flow, *Journal of Fluids and Structures*, Vol. 1, 1987, pp. 239-261.

[2] Zdravkovich, M.M. and Pridden, D.L., Interference between two circular cylinders; series of unexpected discontinuities, *Journal of Industrial Aerodynamics*, Vol. 2, 1977, pp. 255-270.

[3] Price, S.J. and Paidoussis, M.P., The aerodynamic forces acting on groups of two and three circular cylinders when subject to a cross-flow, *Journal of Wind Engineering and Industrial Aerodynamics*, Vol. 17, 1984, pp. 329-347.

[4] Nebres, J. and Batill, S., Flow about a circular cylinder with single large-scale surface perturbation, *Experiments in Fluids*, Vol. 15, 1993 pp. 369-379.

[5] Alam, M. M., Sakamoto, H. and Moriya, M., Reduction of fluid forces acting on a single circular cylinder and two circular cylinders by using tripping rods, *Journal of Fluids and Structures*, Vol. 18, 2003, pp. 347-366.

[6] Alam, M.M., Sakamoto, H. and Zhou, Y., Determination of flow configurations and fluid forces acting on fwo staggered cylinders of equal diameter in cross-flow, *Journal of Fluids and Structures*, Vol. 21, 2005, pp. 363-394.

[7] Alam, M.M., Moriya, M. and Sakamoto, H., Aerodynamic characteristics of two side-by-side circular cylinders and application of wavelet analysis on the switching phenomenon, *Journal Fluids and Structures*, Vol. 18 2003, pp. 325-346.

[8] Alam, M.M. and Sakamoto, H., Investigation of Strouhal frequencies of two staggered bluff bodies and detection of multistable flow by wavelets, *Journal Fluids and Structures*, Vol. 20, 2005, pp. 425-449.

[9] Alam, M.M., Moriya, M., Takai, K. and Sakamoto, H., Fluctuating fluid forces acting on two circular cylinders in a tandem arrangement at a subcritical Reynolds number, *Journal of Wind Engineering and Industrial Aerodynamics*, Vol. 91, 2003, pp. 139-154.